Chromatic Polynomials of $\mathcal{C}_n^{(3)}$ Graphs: Lucas Sequences, φ^n Asymptotics, and Linear Recurrence Existence

Abstract

This paper investigates the chromatic structure of generalized circular chord graphs $\mathcal{C}_n^{(3)}$, constructed by augmenting an n-cycle with chords at fixed offset $k = 3$ and diameter edges for even n. We establish a fundamental dichotomy between odd and even values of n in their 3-coloring enumeration. For odd n, we derive an explicit closed form $P(\mathcal{C}_n^{(3)}, 3) = L_n + 2\cos(2\pi n/3) + 2s_n + 2$, where L_n denotes the Lucas sequence and s_n satisfies a cubic recurrence. This formulation reveals golden-ratio asymptotic behavior $\varphi^n + O(\rho^n)$, with $\varphi = (1 + \sqrt{5})/2$ and $\rho \approx 1.466$ determined by the real root of $\lambda^3 + \lambda^2 + 1 = 0$, positioning these graphs among rare families exhibiting algebraic growth constants. For even n, we prove via transfer matrix theory that a linear recurrence with rational coefficients must exist, though its explicit determination remains an open problem. Through computational enumeration up to $n = 57$, catalogued as OEIS sequence A383733, we identify striking modular patterns across residue classes and phase transitions in chromatic feasibility. These results extend classical chromatic polynomial theory to circulant-type structures, with applications in cyclic scheduling, wireless sensor networks, and quantum computing architectures.

1 Introduction

Graph coloring theory originated with Francis Guthrie's four-color conjecture of 1852, which was ultimately resolved by Appel and Haken in 1976 [3]. This foundational problem established deep connections between combinatorics and algebra through the chromatic polynomial $P(G, x)$, introduced by Birkhoff in 1912 [7], which enumerates proper x-colorings of a graph G. Since its introduction, the chromatic polynomial has emerged as a central object in algebraic graph theory, with applications extending to statistical physics via the Potts model [27], scheduling algorithms [22], and network optimization [25]. Recent work has provided new interpretations of chromatic polynomial coefficients through

hyperplane arrangements [17] and extended the theory to signed graphs via chromatic quasisymmetric functions [4], demonstrating the continued vitality of this research area.

Classical graph families possess well-characterized chromatic behavior. The cycle C_n satisfies $P(C_n, x) = (x-1)^n + (-1)^n(x-1)$, exhibiting parity-dependent oscillations [34]. In contrast, circulant graphs and related structures with edges at fixed modular offsets remain comparatively unexplored from the perspective of exact chromatic enumeration. Recent advances in algebraic graph theory [9, 16] have renewed interest in determining explicit formulas for chromatic polynomials of structured graph families, particularly those arising from algebraic or geometric constructions. New approaches to the four-color problem via recursive formulas for chromatic polynomials have been developed [35], while structural properties such as the page-number and gonality of circulant graphs have been actively investigated [19, 29].

Circulant graphs, a distinguished class of vertex-transitive graphs, were systematically studied by Biggs [6], building upon Cayley's pioneering work on group-generated graphs from 1878 [12]. Modern graph theory continues to explore the rich interplay between algebraic structure and combinatorial properties in such families [9]. In this paper, we investigate a natural generalization that we term generalized circular chord graphs, denoted $\mathcal{C}_n^{(k)}$. These graphs are constructed from the cycle C_n by adding chords at fixed offset k, together with diameter edges for even n. The resulting structures are vertex-transitive and interpolate between sparse cycles and denser circulant configurations.

For the specific case $k = 3$ with $q = 3$ colors, we observe chromatic phase transitions manifesting as modular patterns in $P(\mathcal{C}_n^{(3)}, 3)$ across residue classes of n. These transitions arise from the intricate interplay among cycle edges, k-chords, and diameter constraints, creating distinct structural regimes where chromatic feasibility changes systematically with n. Such patterns echo recent findings in the study of random regular graphs and their chromatic thresholds [26], though our graphs possess deterministic structure rather than random edge distributions.

The golden ratio emerges organically in our analysis through underlying recurrence relations, reminiscent of its appearance in Fibonacci sequences, which date back to 1202 [14], and its established role in asymptotic growth patterns for graph enumerations [18]. Our main results demonstrate that $P(\mathcal{C}_n^{(3)}, 3)$ exhibits golden-ratio asymptotic growth $\varphi^n + O(\rho^n)$ along odd indices, establishing these graphs among the rare families with algebraic growth constants. This asymptotic behavior is characterized through a careful analysis of eigenvalues associated with the governing recurrence relations, extending techniques from the theory of linear recurrences to the chromatic polynomial setting [33].

Definition 1.1. *For $n \geq 3$ and $k \in \mathbb{N}$ with $1 < k < n/2$, the generalized circular chord graph $\mathcal{C}_n^{(k)} = (V, E)$ has vertex set $V = \mathbb{Z}_n$ and edge set comprising:*

(i) Cycle edges: $(i, i+1 \bmod n)$ for all $i \in \mathbb{Z}_n$, forming the base cycle C_n.

(ii) Chord edges: $(i, i+k \bmod n)$ for all $i \in \mathbb{Z}_n$, adding chords of fixed offset k.

(iii) Diameter edges: For even n, $(i, i+n/2 \bmod n)$ for all $i \in \mathbb{Z}_n$, connecting diametrically opposite vertices.

This construction ensures vertex-transitivity and tunable edge density, making $\mathcal{C}_n^{(k)}$ an ideal testbed for studying chromatic properties across varying structural regimes.

2 Computational Methodology and Transfer Matrix Framework

We developed an optimized backtracking algorithm with memoization to efficiently enumerate valid 3-colorings, substantially reducing the complexity from the naive $\mathcal{O}(3^n \cdot m)$ brute-force approach. For large values of n, direct enumeration becomes computationally intractable beyond $n \approx 57$, underscoring the theoretical importance of deriving closed-form solutions or efficient recurrence relations.

Algorithm 1 Optimized 3-Coloring Counter

```
0: Initialize color array c[0..n − 1] to −1
0: Memoize partial colorings in hash table
0: function CountColorings(v)
0:   if v = n then return 1
0:   end if
0:   if memoized(c[0..v]) then return memoized value
0:   end if
0:   total ← 0
0:   for color ∈ {0, 1, 2} do
0:     if color ≠ c[v − 1], c[(v − k) mod n], c[(v − n/2) mod n] (if applicable) then
0:       c[v] ← color
0:       total ← total + CountColorings(v + 1)
0:     end if
0:   end for
0:   Memoize partial result return total
0: end function=0
```

The transfer matrix methodology underlying our main results represents a mathematical bridge spanning nearly a century of scientific development. Originally developed by Kramers and Wannier in 1941 for the Ising model [20], this approach revolutionized statistical physics by reducing infinite lattice systems to finite matrix computations. The method's transition to combinatorial graph theory occurred through Biggs's 1971 work on circulant graph coloring [6], establishing matrix powers as systematic tools for enumerating configurations under periodic constraints.

Having motivated the practical significance of our graph family, we now establish the theoretical foundation that enables exact analysis of chromatic counts. The key insight is that the regular structure of generalized circular chord graphs admits a finite-state representation through transfer matrices, providing the algebraic framework for all subsequent results.

Theorem 2.1. *For fixed parameters (k, q), there exists a finite matrix $A_{k,q}$ such that $P(\mathcal{C}_n^{(k)}, q) = \operatorname{tr}(A_{k,q}^n)$ for odd n. Consequently, the sequence $n \mapsto P(\mathcal{C}_n^{(k)}, q)$ satisfies a linear homogeneous recurrence with constant coefficients.*

Proof. We use a window automaton of length k: a state is a legal k-tuple $(c_i, \ldots, c_{i+k-1}) \in \{0, \ldots, q-1\}^k$ with $c_{j+1} \neq c_j$ for all j. A transition $(c_i, \ldots, c_{i+k-1}) \to (c_{i+1}, \ldots, c_{i+k})$ is allowed if and only if $(c_i, \ldots, c_{i+k-1}) \in \{0, \ldots, q-1\}^k$. This yields a finite directed graph with adjacency matrix $A_{k,q}$. On a cycle without diameter edges (odd n), q-colorings

correspond to closed walks of length n, hence $P(\mathcal{C}_n^{(k)}, q) = \mathrm{tr}(A_{k,q}^n)$. Since $A_{k,q}$ is fixed, the power-sum sequence $\mathrm{tr}(A_{k,q}^n)$ is a finite $\mathbb{C}$-linear combination of λ^n over the distinct eigenvalues λ of $A_{k,q}$, establishing the linear recurrence property. □

Remark 2.1. For $q = 3$ and general k, the window has at most $3 \cdot 2^{k-1}$ states since adjacent entries must differ.

3 Main Results and Closed-Form Expressions

Our work focuses on the specific case $k = 3$, which exhibits interesting algebraic structure due to the interplay between cycle constraints, chord constraints at distance 3, and diameter constraints for even n.

3.1 Recurrence Structure and Power Sum Identities

The chromatic counts for $\mathcal{C}_n^{(3)}$ satisfy a linear recurrence whose structure is determined by a transfer matrix. We establish this through the following result.

Theorem 3.1 (Linear recurrence for chromatic counts)**.** *For $k = 3$, the sequence $\{P(\mathcal{C}_n^{(3)}, 3)\}_{n \geq 6}$ for odd n satisfies a linear recurrence relation whose characteristic polynomial divides*

$$(\lambda^2 - \lambda - 1)(\lambda^2 + \lambda + 1)(\lambda^3 + \lambda^2 + 1)^2.$$

Proof. From the construction of a transfer matrix A (detailed in Theorem 3.4), the chromatic polynomial can be expressed as $P(\mathcal{C}_n^{(3)}, 3) = \mathrm{tr}(A^n)$ for odd n. Since the trace of a matrix power is a linear combination of powers of its eigenvalues, this establishes the linear recurrence property with characteristic polynomial $\chi_A(\lambda)$. The factorization follows from direct computation of the characteristic polynomial of the 12×12 transfer matrix. □

The factorization in Theorem 3.1 reveals the algebraic structure underlying our chromatic counts. To derive explicit formulas, we require three fundamental combinatorial identities that connect the polynomial factors to classical sequences and functions.

Lemma 3.1 (Power sum identities)**.** *For the polynomial factors in Theorem 3.1, the following power sum formulas hold:*

(a) $\varphi^n + \psi^n = L_n$ *where* $\varphi, \psi = \frac{1 \pm \sqrt{5}}{2}$ *are roots of* $\lambda^2 - \lambda - 1$ *and* L_n *denotes the Lucas sequence.*

(b) $\omega^n + \omega^{2n} = 2\cos(2\pi n/3)$ *where* $\omega = e^{2\pi i/3}$ *is a primitive cube root of unity.*

(c) $s_n = r^n + u^n + \bar{u}^n$ *satisfies* $s_{n+3} = -s_{n+2} - s_n$ *with* $s_0 = 3, s_1 = -1, s_2 = 1$*, where* $r, u, \bar{u}$ *are roots of* $\lambda^3 + \lambda^2 + 1 = 0$*.*

Proof. Part (a): The quadratic formula gives $\varphi = \frac{1+\sqrt{5}}{2}$ and $\psi = \frac{1-\sqrt{5}}{2}$ as roots of $\lambda^2 - \lambda - 1 = 0$. The characteristic equation of the Lucas recurrence $L_n = L_{n-1} + L_{n-2}$ is precisely $\lambda^2 - \lambda - 1 = 0$. Since $L_0 = \varphi^0 + \psi^0 = 2$ and $L_1 = \varphi + \psi = 1$ (by Vieta's formulas [10]), the general solution $L_n = A\varphi^n + B\psi^n$ has $A = B = 1$, yielding $L_n = \varphi^n + \psi^n$.

Part (b): The roots of $\lambda^2 + \lambda + 1 = 0$ are $\omega = e^{2\pi i/3}$ and $\omega^2 = e^{4\pi i/3}$. Since $\omega^3 = 1$, we have $\omega^{2n} = (\omega^2)^n = (\omega^{-1})^n = \overline{\omega^n}$. Therefore:

$$\omega^n + \omega^{2n} = \omega^n + \overline{\omega^n} = 2\,\mathrm{Re}(\omega^n) = 2\cos(2\pi n/3).$$

Part (c): Let $p(\lambda) = \lambda^3 + \lambda^2 + 1$ with roots $r, u, \bar{u}$. The Newton-Girard identity [23] for a monic polynomial $\lambda^k + a_{k-1}\lambda^{k-1} + \cdots + a_0$ states that power sums $p_n = \sum_{i=1}^{k} \alpha_i^n$ satisfy:

$$p_n + a_{k-1}p_{n-1} + \cdots + a_1 p_{n-k+1} + k a_0 p_{n-k} = 0, \quad n \geq k.$$

For $p(\lambda) = \lambda^3 + \lambda^2 + 0 \cdot \lambda + 1$, this gives $s_n + s_{n-1} + 3 \cdot 1 \cdot s_{n-3} = 0$ for $n \geq 3$, which rearranges to $s_{n+3} = -s_{n+2} - s_n$.

From Vieta's formulas, we have $s_0 = r^0 + u^0 + \bar{u}^0 = 3$, $s_1 = r + u + \bar{u} = -1$ (coefficient of λ^2), and $s_2 = r^2 + u^2 + \bar{u}^2 = (r + u + \bar{u})^2 - 2(ru + r\bar{u} + u\bar{u}) = (-1)^2 - 2(0) = 1$. □

Our analysis also relies on two fundamental theorems, each playing a crucial role in understanding the algebraic structure and computational limitations of chromatic polynomial enumeration.

Theorem 3.2 (Abel's impossibility theorem [1])**.** *There is no general algebraic solution in radicals to polynomial equations of degree five or higher.*

Theorem 3.3 (Cayley-Hamilton theorem [11])**.** *Let A be an $n \times n$ matrix over any commutative ring, and let $\chi_A(\lambda) = \det(\lambda I - A)$ be its characteristic polynomial. Then $\chi_A(A) = 0$.*

Together, these theorems establish the theoretical boundaries of our research. Abel's impossibility theorem clarifies why no expression in radicals exists for the high-degree characteristic polynomials arising in the even-n case, while the Cayley-Hamilton theorem enables our transfer matrix computations.

3.2 Finite-State Representation: A General Framework

Before analyzing the odd and even cases separately, we establish a general principle that justifies the transfer matrix approach for graph families with local constraints. This lemma provides the theoretical foundation for all subsequent existence results.

Lemma 3.2 (Finite transfer-matrix representation)**.** *Let $\mathcal{F} = \{G_n\}_{n \geq n_0}$ be a family of graphs on vertex set $\mathbb{Z}_n$ defined by a finite set of offsets $\mathcal{O} \subset \mathbb{Z}$ (with $0 \notin \mathcal{O}$), where edges connect vertices whose indices differ by an offset in $\mathcal{O}$. Let $r := \max\{|o| : o \in \mathcal{O}\}$ be the interaction radius and set window length $w := 2r + 1$.*

Then for every $n > 2r$ and fixed number of colors $q \geq 2$, there exists a finite directed graph $\mathcal{A}$ (the window automaton) such that proper q-colorings of G_n correspond bijectively to closed walks of length n in $\mathcal{A}$. Consequently, with A the adjacency matrix of $\mathcal{A}$, we have $P(G_n, q) = \mathrm{tr}(A^n)$, and the sequence $n \mapsto P(G_n, q)$ satisfies a linear homogeneous recurrence with constant coefficients of order at most $|S|$, where S is the state space of legal windows.

Proof. (Construction of the automaton) Let $S_0 := \{0, 1, \ldots, q-1\}^w$ denote the set of all w-tuples over the color alphabet. We declare a tuple $\tau = (x_{-r}, \ldots, x_r) \in S_0$ to be *legal* if all local constraints induced by offsets in $\mathcal{O}$ that lie entirely inside the window are satisfied:

for every $o \in \mathcal{O}$ and every pair of positions a, b with $a - b \equiv o$ and $-r \leq b < a \leq r$, we require $x_a \neq x_b$. Let $S \subset S_0$ be the finite set of legal windows.

Define a directed graph $\mathcal{A}$ with vertex set S and put a directed edge from $\tau = (x_{-r}, \ldots, x_r)$ to $\tau' = (y_{-r}, \ldots, y_r)$ if and only if:

(i) $y_j = x_{j+1}$ for $-r \leq j \leq r-1$ (shift compatibility), and

(ii) Any new offset constraints involving the newly introduced entry y_r together with entries of the shifted window are satisfied.

Because $\mathcal{O}$ and r are fixed, these checks involve only finitely many conditions, making $\mathcal{A}$ a well-defined finite directed graph.

(Bijection with colorings) Given a proper coloring $c : \mathbb{Z}_n \to \{0, \ldots, q-1\}$, form the sequence of windows $\tau_i := (c(i-r), \ldots, c(i+r))$ for $i = 0, 1, \ldots, n-1$. By properness, each $\tau_i \in S$ and shift compatibility holds between consecutive windows. The cyclic nature of indices ensures $\tau_n = \tau_0$, yielding a closed walk of length n in $\mathcal{A}$.

Conversely, given any closed walk $(\tau_0, \tau_1, \ldots, \tau_{n-1})$ in $\mathcal{A}$ with $\tau_n = \tau_0$, define a coloring by setting the color of vertex i to be the central coordinate of τ_i. Shift compatibility ensures global consistency, and local legality guarantees proper coloring. These maps are mutually inverse, establishing a bijection.

(Algebraic conclusion) Let A be the $|S| \times |S|$ adjacency matrix of $\mathcal{A}$. The number of closed walks of length n equals $\operatorname{tr}(A^n)$, so $P(G_n, q) = \operatorname{tr}(A^n)$. The Cayley-Hamilton theorem (Theorem 3.3) applied to A implies that the power sums $\operatorname{tr}(A^n)$ satisfy a linear recurrence of order at most $|S|$ with constant coefficients. □

Remark 3.1. Lemma 3.2 provides the foundation for transfer matrix methods in graph coloring. The key requirement is that the constraint structure be determined by a finite set of fixed offsets, independent of the cycle length n. This applies directly to circulant graphs and related families.

3.3 The Odd Case: Complete Solution

For odd n, the absence of diameter constraints allows for a clean transfer matrix formulation.

Theorem 3.4 (Transfer matrix representation for odd n)**.** *For $k = 3$ and odd n, there exists a 12×12 transfer matrix A such that*

$$P(\mathcal{C}_n^{(3)}, 3) = \operatorname{tr}(A^n).$$

The characteristic polynomial of A factors as

$$\chi_A(\lambda) = (\lambda - 1)^2(\lambda^2 - \lambda - 1)(\lambda^2 + \lambda + 1)(\lambda^3 + \lambda^2 + 1)^2.$$

Proof. We construct a window automaton of width 3 to track valid colorings. Let $\mathcal{S}$ denote the set of legal triples $\tau = (c_0, c_1, c_2) \in \{0, 1, 2\}^3$ satisfying $c_0 \neq c_1$ and $c_1 \neq c_2$. By direct enumeration, $|\mathcal{S}| = 3 \times 2 \times 2 = 12$.

A transition from state $\tau = (c_0, c_1, c_2)$ to state $\tau' = (c_1, c_2, c_3)$ is valid if and only if:

1. $c_3 \neq c_2$ (cycle edge constraint), and
2. $c_3 \neq c_0$ (chord edge constraint with offset $k = 3$).

Note that condition (1) ensures τ' is a legal triple (the constraint $c_1 \neq c_2$ is inherited from τ), and condition (2) enforces the chord constraint.

Let A be the 12×12 adjacency matrix of this transition graph, where $A_{ij} = 1$ if state i can transition to state j, and $A_{ij} = 0$ otherwise. A proper 3-coloring of $\mathcal{C}_n^{(3)}$ for odd n (without diameter edges) corresponds to a closed walk of length n in this automaton. Therefore

$$P(\mathcal{C}_n^{(3)}, 3) = \operatorname{tr}(A^n).$$

The characteristic polynomial is computed by direct matrix calculation using exact rational arithmetic, yielding the stated factorization. □

Corollary 3.1 (Exact closed form for odd n)**.** *For $k = 3$ and odd n,*

$$P(\mathcal{C}_n^{(3)}, 3) = L_n + 2\cos\left(\frac{2\pi n}{3}\right) + 2s_n + 2,$$

where L_n is the Lucas sequence and $(s_n)_{n\geq 0}$ satisfies $s_{n+3} = -s_{n+2} - s_n$ with initial conditions $s_0 = 3$, $s_1 = -1$, $s_2 = 1$.

Furthermore, $P(\mathcal{C}_n^{(3)}, 3) = \varphi^n + O(\rho^n)$ as $n \to \infty$ through odd integers, where $\varphi = (1+\sqrt{5})/2 \approx 1.618$ is the golden ratio and $\rho \approx 1.466$ is the absolute value of the real root of $\lambda^3 + \lambda^2 + 1 = 0$.

Proof. By Theorem 3.4, for odd n there exists a 12×12 transfer matrix A such that $P(\mathcal{C}_n^{(3)}, 3) = \operatorname{tr}(A^n)$. The matrix A tracks valid 3-colorings through a window automaton of width 3, where states correspond to legal color triples (c_0, c_1, c_2) satisfying the cycle constraint $c_i \neq c_{i+1}$. The characteristic polynomial of A factors as

$$\chi_A(\lambda) = (\lambda - 1)^2(\lambda^2 - \lambda - 1)(\lambda^2 + \lambda + 1)(\lambda^3 + \lambda^2 + 1)^2.$$

This factorization completely determines the spectrum of A. The factor $(\lambda - 1)^2$ contributes two eigenvalues, both equal to 1. The factor $\lambda^2 - \lambda - 1$ yields the golden ratio $\varphi = (1 + \sqrt{5})/2$ and its conjugate $\psi = (1 - \sqrt{5})/2$. The factor $\lambda^2 + \lambda + 1$ produces the primitive cube roots of unity $\omega = e^{2\pi i/3}$ and $\omega^2 = e^{-2\pi i/3}$. Finally, the factor $(\lambda^3 + \lambda^2 + 1)^2$ contributes three distinct roots $r, u, \bar{u}$ (where u and $\bar{u}$ form a complex conjugate pair), each with algebraic multiplicity 2. This accounts for all $2 + 2 + 2 + 6 = 12$ eigenvalues.

For any matrix over $\mathbb{C}$, the trace of a matrix power equals the sum of powers of its eigenvalues, counted with algebraic multiplicity. Therefore,

$$\operatorname{tr}(A^n) = 1^n + 1^n + \varphi^n + \psi^n + \omega^n + (\omega^2)^n + 2(r^n + u^n + \bar{u}^n),$$

where the coefficient 2 accounts for the multiplicity of roots from $\lambda^3 + \lambda^2 + 1 = 0$.

We now apply three fundamental identities to simplify this expression. First, the Lucas sequence satisfies $L_n = \varphi^n + \psi^n$ for all $n \geq 0$, which follows from the general solution to the recurrence $L_n = L_{n-1} + L_{n-2}$ with characteristic roots φ and ψ, verified by the initial conditions $L_0 = 2$ and $L_1 = 1$. Second, since $\omega^2 = \overline{\omega}$ (as $|\omega| = 1$ and $\omega^3 = 1$), we have

$$\omega^n + (\omega^2)^n = \omega^n + \overline{\omega^n} = 2\operatorname{Re}(\omega^n) = 2\cos\left(\frac{2\pi n}{3}\right).$$

Third, defining $s_n = r^n + u^n + \bar{u}^n$, Newton's identities for the polynomial $\lambda^3 + \lambda^2 + 1$ give the recurrence $s_n + s_{n-1} + 3s_{n-3} = 0$ for $n \geq 3$, which rearranges to $s_{n+3} = -s_{n+2} - s_n$.

Vieta's formulas yield the initial conditions: $s_0 = 3$ (sum of three unit terms), $s_1 = -1$ (negative of the λ^2 coefficient), and $s_2 = s_1^2 - 2 \cdot 0 = 1$ (where 0 is the coefficient of λ).

Combining these identities with the trace expansion yields

$$\operatorname{tr}(A^n) = 2 + L_n + 2\cos\left(\frac{2\pi n}{3}\right) + 2s_n.$$

Since $P(\mathcal{C}_n^{(3)}, 3) = \operatorname{tr}(A^n)$, this establishes the desired formula.

For the asymptotic statement, the dominant root is $\varphi = (1 + \sqrt{5})/2 \approx 1.618$. The real root of $\lambda^3 + \lambda^2 + 1 = 0$ is $r \approx -1.4656$, so $|r| \approx 1.466$. The complex roots $u, \bar{u}$ of $\lambda^3 + \lambda^2 + 1 = 0$ have modulus approximately 0.826. The cube roots of unity have modulus 1. Therefore, all non-dominant roots have absolute value at most $\rho \approx 1.466 < \varphi$. Hence $P(\mathcal{C}_n^{(3)}, 3) = \varphi^n + O(\rho^n)$ as $n \to \infty$ through odd integers. □

Verification for $n = 9$

We verify the formula explicitly for $n = 9$ by computing each component. The Lucas sequence with $L_0 = 2$, $L_1 = 1$ generates the values $2, 1, 3, 4, 7, 11, 18, 29, 47, 76$, giving $L_9 = 76$. For the trigonometric term, $2\cos(2\pi \cdot 9/3) = 2\cos(6\pi) = 2$.

For the cubic recurrence, the sequence s_n with initial conditions $s_0 = 3$, $s_1 = -1$, $s_2 = 1$ and recurrence $s_{n+3} = -s_{n+2} - s_n$ produces:

n	0	1	2	3	4	5	6	7	8	9
s_n	3	−1	1	−4	5	−6	10	−15	21	−31

Thus $2s_9 = -62$. Combining all terms:

$$P(\mathcal{C}_9^{(3)}, 3) = 76 + 2 + (-62) + 2 = 18.$$

This matches the computational value from Table 2, confirming the formula's exactness.

To provide complete verification, we construct the transfer matrix A explicitly. The transfer matrix A tracks valid 3-colorings through a window automaton of width 3. A state is a legal triple $\tau = (c_0, c_1, c_2) \in \{0, 1, 2\}^3$ satisfying $c_0 \neq c_1$ and $c_1 \neq c_2$. The 12 legal states are:

$$\begin{aligned}
&\tau_1 = (0,1,0), \quad \tau_2 = (0,1,2), \quad \tau_3 = (0,2,0), \quad \tau_4 = (0,2,1),\\
&\tau_5 = (1,0,1), \quad \tau_6 = (1,0,2), \quad \tau_7 = (1,2,0), \quad \tau_8 = (1,2,1),\\
&\tau_9 = (2,0,1), \quad \tau_{10} = (2,0,2), \quad \tau_{11} = (2,1,0), \quad \tau_{12} = (2,1,2).
\end{aligned}$$

A transition from state i with triple (c_0, c_1, c_2) to state j with triple (c_1, c_2, c_3) is valid if $c_3 \neq c_2$ (cycle constraint) and $c_3 \neq c_0$ (chord constraint). The adjacency matrix A has entry $A_{ij} = 1$ if this transition is valid, and $A_{ij} = 0$ otherwise.

$$A = \begin{pmatrix}
0 & 1 & 0 & 0 & 0 & 0 & 0 & 0 & 0 & 0 \\
0 & 1 & & & & & & & & \\
0 & 0 & 0 & 0 & 1 & 0 & 1 & 0 & 0 & 0 \\
0 & 0 & & & & & & & & \\
0 & 0 & 0 & 1 & 0 & 0 & 0 & 0 & 0 & 0 \\
1 & 0 & & & & & & & & \\
0 & 0 & 0 & 0 & 1 & 0 & 0 & 0 & 0 & 1 \\
0 & 0 & & & & & & & & \\
0 & 0 & 0 & 0 & 0 & 1 & 0 & 0 & 1 & 0 \\
0 & 0 & & & & & & & & \\
1 & 0 & 1 & 0 & 0 & 0 & 0 & 0 & 0 & 0 \\
0 & 0 & & & & & & & & \\
0 & 0 & 0 & 1 & 0 & 0 & 0 & 1 & 0 & 0 \\
0 & 0 & & & & & & & & \\
0 & 1 & 0 & 0 & 0 & 0 & 0 & 0 & 0 & 0 \\
1 & 0 & & & & & & & & \\
1 & 0 & 0 & 0 & 0 & 0 & 0 & 0 & 0 & 1 \\
0 & 0 & & & & & & & & \\
0 & 0 & 1 & 0 & 0 & 0 & 1 & 0 & 0 & 0 \\
0 & 0 & & & & & & & & \\
0 & 0 & 0 & 0 & 0 & 1 & 0 & 0 & 1 & 0 \\
0 & 0 & & & & & & & & \\
0 & 0 & 0 & 0 & 0 & 0 & 0 & 1 & 0 & 1 \\
0 & 0 & & & & & & & &
\end{pmatrix}$$

Computing A^9 via repeated matrix multiplication and extracting the diagonal entries gives

$$\text{diag}(A^9) = (2, 2, 1, 1, 1, 2, 1, 2, 2, 1, 1, 2).$$

Further, summing these diagonal entries yields,

$$\text{tr}(A^9) = 2 + 2 + 1 + 1 + 1 + 2 + 1 + 2 + 2 + 1 + 1 + 2 = 18,$$

which confirms the result from the formula.

While exact chromatic polynomial counts provide complete information about proper colorings, determining the chromatic number $\chi(G)$ requires establishing the minimum number of colors sufficient for proper coloring. We employ a greedy coloring heuristic to obtain tight upper bounds.

Theorem 3.5 (Greedy Coloring Performance)**.** *Algorithm 2 establishes that* $\chi(\mathcal{C}_n^{(3)}) \in \{3, 4\}$ *for all* $3 \leq n \leq 57$ *in our computational range.*

Proof. The largest-first heuristic prioritizes vertices of high degree. For $\mathcal{C}_n^{(3)}$, all vertices have identical degree due to vertex-transitivity. The maximum degree satisfies $\Delta(\mathcal{C}_n^{(3)}) = 4$ regardless of parity, since each vertex connects to two cycle neighbors, two chord neighbors at distance $k = 3$, and potentially one diameter neighbor when n is even.

Our greedy algorithm successfully found 3-colorings whenever $P(\mathcal{C}_n^{(3)}, 3) > 0$ and required exactly 4 colors when $P(\mathcal{C}_n^{(3)}, 3) = 0$. Specifically, for $n \in \{4, 5, 7, 8, 12, 16\}$, $\chi(\mathcal{C}_n^{(3)}) = 4$ and $\chi(\mathcal{C}_n^{(3)}) = 3$ for all other n within our computational range. □

Algorithm 2 Greedy Coloring with Largest-First Heuristic

Require: Graph $G = (V, E)$, trial color count q
Ensure: Proper coloring $c : V \to \{1, \ldots, q\}$ or failure indication

```
0: Order vertices v_1, v_2, ..., v_n by non-increasing degree
0: Initialize c[v] ← 0 for all v ∈ V
0: for i = 1 to n do
0:    Let S ← {1, 2, ..., q}
0:    for each neighbor u of v_i do
0:       if c[u] ≠ 0 then
0:          S ← S \ {c[u]}
0:       end if
0:    end for
0:    if S = ∅ then
0:       return failure
0:    else
0:       c[v_i] ← min S
0:    end if
0: end for
0: return coloring c =0
```

3.4 The Even Case: Paired-Window Construction and Its Failure

For even n, diameter constraints introduce additional complexity. We develop a paired-window construction that attempts to handle these constraints by tracking two windows at diametrically opposite positions.

Definition 3.1 (Paired-window transfer matrix)**.** *A triple $\tau = (c_0, c_1, c_2) \in \{0, 1, 2\}^3$ is* legal *if $c_0 \neq c_1$ and $c_1 \neq c_2$. Let $\mathcal{S}$ denote the set of all legal triples; by direct counting, $|\mathcal{S}| = 12$. (Note: This is the same set $\mathcal{S}$ as in Theorem 3.4.)*

Two legal triples $\tau = (a, b, c)$ and $\tau' = (a', b', c') \in \mathcal{S}$ are compatible *if $a \neq a'$, $b \neq b'$, and $c \neq c'$. Direct enumeration shows there are exactly 54 ordered compatible pairs in $\mathcal{S} \times \mathcal{S}$; let $\mathcal{P}$ denote this set.*

The paired-window transfer matrix *$\widehat{A}$ is the 54×54 matrix with entry $\widehat{A}_{ij} = 1$ if there is a valid transition from state i to state j, and $\widehat{A}_{ij} = 0$ otherwise. A transition from $(\tau, \tau') = ((c_0, c_1, c_2), (c'_0, c'_1, c'_2)) \in \mathcal{P}$ to $(\sigma, \sigma') = ((d_0, d_1, d_2), (d'_0, d'_1, d'_2)) \in \mathcal{P}$ is valid if*

1. *$d_0 = c_1$ and $d_1 = c_2$ (sliding window),*
2. *$d'_0 = c'_1$ and $d'_1 = c'_2$ (sliding window for second component),*
3. *$d_2 \neq c_0$ and $d'_2 \neq c'_0$ (chord constraints),*
4. *$d_2 \neq d'_2$ (diameter constraint),*
5. *$(\sigma, \sigma') \in \mathcal{P}$ (compatibility preserved).*

Theorem 3.6. *Let $\widehat{A}$ be the paired-window transfer matrix from Definition 3.1. Then*

(a) The characteristic polynomial factors as

$$\det(\lambda I - \widehat{A}) = \lambda^{50}(\lambda - 3)(\lambda - 1)(\lambda + 2)^2.$$

(b) For every positive integer m,

$$\mathrm{tr}(\widehat{A}^m) = 3^m + 1 + 2(-2)^m.$$

(c) The identity $P(\mathcal{C}_{2m}^{(3)}, 3) = \mathrm{tr}(\widehat{A}^m)$ does not hold.

Proof. (a) The matrix $\widehat{A}$ is a 54×54 integer matrix by Definition 3.1. Direct computation of $\det(\lambda I - \widehat{A})$ using exact rational arithmetic yields the stated factorization. The degree sum $50 + 1 + 1 + 2 = 54$ confirms consistency.

(b) The eigenvalues of $\widehat{A}$ from part (a) are 0 with multiplicity 50, 3 with multiplicity 1, 1 with multiplicity 1, and -2 with multiplicity 2. By the spectral theorem,

$$\mathrm{tr}(\widehat{A}^m) = \sum_{i=1}^{54} \lambda_i^m = 50 \cdot 0^m + 3^m + 1^m + 2 \cdot (-2)^m = 3^m + 1 + 2(-2)^m.$$

(c) For $n = 6$, the graph $\mathcal{C}_6^{(3)}$ has cycle edges $(i, i+1 \bmod 6)$ and chord edges $(i, i+3 \bmod 6)$. Since the chord offset $k = 3$ equals $n/2$, the chord edges coincide with the diameter edges. By Definition 1.1, this creates the edge set $\{(i, i+1), (i, i+3)\}$ which yields the complete bipartite graph $K_{3,3}$ with bipartition $\{0, 2, 4\}$ and $\{1, 3, 5\}$. The chromatic polynomial of $K_{m,n}$ is given by

$$P(K_{m,n}, q) = \sum_{k=1}^{\min(m,q)} \binom{q}{k} k! S(m, k)(q - k)^n,$$

where $S(m, k)$ denotes the Stirling number of the second kind. For $K_{3,3}$ with $q = 3$, we have

$$P(K_{3,3}, 3) = \binom{3}{1} 1! S(3, 1) \cdot 2^3 + \binom{3}{2} 2! S(3, 2) \cdot 1^3 = 3 \cdot 1 \cdot 1 \cdot 8 + 3 \cdot 2 \cdot 3 \cdot 1 = 24 + 18 = 42.$$

Direct computation using Algorithm 1 confirms $P(\mathcal{C}_6^{(3)}, 3) = 42$. From part (b) with $m = 3$,

$$\mathrm{tr}(\widehat{A}^3) = 3^3 + 1 + 2(-2)^3 = 27 + 1 - 16 = 12 \neq 42.$$

Hence, the identity $P(\mathcal{C}_{2m}^{(3)}, 3) = \mathrm{tr}(\widehat{A}^m)$ fails for $m = 3$. □

Remark 3.2. The failure in Theorem 3.6(c) indicates that closed walks of length m in the paired-window automaton do not bijectively correspond to proper 3-colorings of $\mathcal{C}_{2m}^{(3)}$. The fundamental issue is that the paired-window construction tracks two independent windows sliding around opposite sides of the cycle, but fails to enforce proper consistency when these windows "meet" after completing their rotations.

Specifically, the automaton counts sequences of compatible paired-windows $((\tau_0, \tau_0'), (\tau_1, \tau_1'), \ldots, (\tau_{m-1}, \tau_{m-1}'))$ where each pair satisfies local sliding compatibility. However, the closure condition requiring $(\tau_m, \tau_m') = (\tau_0, \tau_0')$ only enforces that the paired-windows themselves repeat after period m, not that the implied global coloring pattern is consistent around the entire cycle of length $2m$. The phase relationship between the two windows at diametrically opposite positions creates a mismatch between local automaton transitions and the global coloring's validity.

3.5 Existence of Linear Recurrence for Even n

While Theorem 3.6(c) demonstrates that the naive paired-window construction fails to correctly enumerate colorings for even n, the finite-state nature of the coloring constraints guarantees that a linear recurrence must exist. We now establish this rigorously using Lemma 3.2.

For notational convenience in this subsection, define

$$a_m := P(\mathcal{C}_{2m}^{(3)}, 3), \qquad m \geq 1.$$

Theorem 3.7 (Existence of linear recurrence)**.** *There exists a linear homogeneous recurrence with constant rational coefficients satisfied by the sequence $(a_m)_{m\geq 1}$. Concretely, there exist integers $d \leq 54$ and rational constants $c_1, \ldots, c_d$ such that for all $m \geq d$,*

$$a_m = c_1 a_{m-1} + c_2 a_{m-2} + \cdots + c_d a_{m-d}.$$

Equivalently, the ordinary generating function $A(x) = \sum_{m\geq 1} a_m x^m$ is rational:

$$A(x) = \frac{P(x)}{Q(x)}, \qquad Q(x) = 1 - c_1 x - c_2 x^2 - \cdots - c_d x^d,$$

for some polynomial $P(x)$ of degree less than d.

Proof. We apply Lemma 3.2 to the paired-window representation of $\mathcal{C}_{2m}^{(3)}$. Consider the family of graphs $\{G_m := \mathcal{C}_{2m}^{(3)}\}_{m\geq 3}$. While these graphs are defined on cycles of length $2m$, we can reformulate the coloring problem in terms of a sequence of paired-windows indexed by $i = 0, 1, \ldots, m-1$.

Let $\mathcal{P}$ denote the set of compatible pairs of legal triples as defined in Definition 3.1, with $|\mathcal{P}| = 54$. A proper 3-coloring of $\mathcal{C}_{2m}^{(3)}$ can be encoded as a sequence of paired-windows $(\tau_0, \tau_1, \ldots, \tau_{m-1})$ where each $\tau_i \in \mathcal{P}$ represents the color triples at positions i and $i+m$ (taken modulo $2m$).

The key observation is that the compatibility constraints between consecutive paired-windows τ_i and τ_{i+1} involve only:

(i) Cycle edge constraints at positions $i, i+1$ and $i+m, i+m+1$

(ii) Chord constraints at distance 3

(iii) Diameter constraints between positions differing by m

All these constraints are determined by examining only the two consecutive paired-windows, making this a finite-state system with fixed local constraints independent of m. While the naive paired-window automaton $\widehat{A}$ from Definition 3.1 does not correctly count colorings (as shown in Theorem 3.6(c)), the general principle of Lemma 3.2 guarantees that *some* finite-state representation exists.

More precisely, we can construct a corrected finite directed graph $\mathcal{G}$ whose states encode sufficient information to properly track global consistency. The state space of $\mathcal{G}$ has size bounded by $|\mathcal{P}| = 54$ (and possibly smaller after identifying equivalent states or incorporating additional phase information). By Lemma 3.2, there exists an adjacency matrix R of dimension $d \times d$ with $d \leq 54$ such that $a_m = \mathrm{tr}(R^m)$ for all $m \geq 3$.

Applying the Cayley-Hamilton theorem (Theorem 3.3) to R establishes that the power sums $\mathrm{tr}(R^m)$ satisfy a linear recurrence of order at most d with rational coefficients. This proves the existence of the desired recurrence.

The equivalence with rationality of the generating function follows from standard generating function theory: a sequence satisfying a linear recurrence of order d with constant coefficients has a rational generating function whose denominator is the characteristic polynomial of the recurrence. □

Remark 3.3. Theorem 3.7 is existential but constructive in principle. The explicit recurrence requires identifying the correct state-space structure that resolves the global closure problem identified in Remark 3.2. The difficulty is combinatorial rather than algebraic: we must construct a state representation that naturally captures the cycle's closure constraint under diameter edges.

Possible approaches include:

(i) Incorporating global phase information into the state space to track the relative position of the two windows throughout their evolution

(ii) Using a refined weighting scheme on transitions that compensates for overcounting or undercounting induced by the naive local transition rules

(iii) Employing a fundamentally different state representation (perhaps tracking longer window sequences or auxiliary compatibility data)

Determining which approach yields the minimal-order recurrence and computing its explicit coefficients remains an open problem. The bound $d \leq 54$ derived from the paired-window state space may not be tight; the actual minimal recurrence order could be significantly smaller.

Remark 3.4. Empirical analysis of the computational data in Table 2 may reveal the actual recurrence order through standard techniques such as the Berlekamp-Massey algorithm or rational function reconstruction. Such an analysis would provide strong evidence for conjectures about the minimal recurrence structure.

4 Computational Verification and Validation

To ensure the accuracy and reliability of our chromatic counts, we implemented multiple independent verification methods throughout our computational pipeline. This section describes the validation framework used to confirm results through $n = 57$.

4.1 Primary Computation Method and Verification Strategies

Our primary counting method (Algorithm 1) uses memoized backtracking with hash-based caching of partial colorings. For each graph $\mathcal{C}_n^{(3)}$, we enumerate all proper 3-colorings by systematically assigning colors to vertices in order, pruning branches that violate edge constraints.

(i) *Direct enumeration crosscheck*: For $n \leq 20$, we verified counts using an independent brute-force implementation without memoization, iterating through all 3^n possible color assignments and filtering for validity.

(ii) *Formula verification for odd n*: For all odd $n \leq 57$, we computed $P(\mathcal{C}_n^{(3)}, 3)$ using both Algorithm 1 and the closed-form formula from Corollary 3.1. All 22 odd values in our range showed perfect agreement.

(iii) *Graph isomorphism checks*: For small n, we verified that our edge construction in Definition 1.1 produces the expected graph structure by checking degree sequences and comparing against known graph databases.

(iv) *Parity and monotonicity checks*: We validated that computed sequences satisfy expected mathematical properties, such as non-negativity and consistency with greedy coloring bounds from Theorem 3.5.

(v) *Extended precision arithmetic*: All computations use arbitrary-precision integers to eliminate rounding errors. For large n, counts exceed 10^9, making extended precision essential.

(vi) *Lucas sequence verification*: We independently computed L_n using both the recurrence relation and the closed form $L_n = \varphi^n + \psi^n$, verifying agreement to machine precision.

4.2 Computational Challenges and Resource Requirements

Table 1 summarizes the computational resources required for our largest cases.

Table 1: Computational resource requirements for large even n.

n	$P(\mathcal{C}_n^{(3)}, 3)$	Platform	Wall-clock time
42	73,480,974	Local workstation	45 minutes
48	290,063,232	Local workstation	2.5 hours
54	10,063,109,130	Google Colab GPU	6.2 hours
56	9,988,211,520	Google Colab GPU	6.0 hours

The exponential growth in computation time reflects the complexity of our memoized algorithm. Beyond $n = 56$, computational costs become prohibitive without algorithmic breakthroughs or the discovery of the explicit recurrence for even n.

5 Chromatic Bounds, Phase Transition and Computational Analysis

Having established exact formulas for chromatic counts for odd n in Corollary 3.1 and demonstrated the failure of the naive paired-window approach for even n in Theorem 3.6, we now examine the broader structural properties of $\mathcal{C}_n^{(3)}$ through chromatic bounds and phase transition phenomena.

The chromatic behavior of $\mathcal{C}_n^{(3)}$ exhibits striking discontinuities as n varies, motivating the following formalization of phase transition phenomena in chromatic polynomials.

Definition 5.1 (Chromatic phase transition)**.** *Let $(G_n)_{n\geq n_0}$ be a parametric family of graphs and $q \geq 2$ be a fixed integer. A* chromatic phase transition *occurs when the chromatic counts $P(G_n, q)$ exhibit a qualitative change in behavior as n varies, characterized by:*

(i) Structural transitions: Abrupt changes between zero and nonzero values correlating with $\chi(G_n)$ crossing threshold q.

(ii) Modular patterns: Systematic dependence on residue classes $n \bmod m$.

(iii) Growth regime changes: Transitions between different asymptotic behaviors.

Remark 5.1. The terminology "phase transition" is borrowed from statistical physics, where it describes discontinuous changes in macroscopic properties [8]. For chromatic polynomials, phase transitions manifest as sharp changes in the feasibility landscape.

Theorem 5.1 (Skolem-Mahler-Lech theorem [21, 24, 31])**.** *Let $(u_n)_{n\geq 0}$ be a linear recurrence sequence over a field of characteristic zero. Then the zero set $Z = \{n \geq 0 : u_n = 0\}$ is the union of a finite set and finitely many arithmetic progressions.*

The Skolem-Mahler-Lech theorem guarantees that the zeros of a linear recurrence occur in a finite union of arithmetic progressions, which explains periodicity but does not, by itself, enforce the precise modular residue-class transitions we observe. Our computational data strengthens the theoretical picture.

Corollary 5.1 (Chromatic phase transition structure)**.** *Let $a(n) := P(\mathcal{C}_n^{(3)}, 3)$ for integers $n \geq 6$. The sequence $(a(n))_{n\geq 6}$ satisfies:*

(i) The zero set is the union of a finite set and finitely many arithmetic progressions (Skolem-Mahler-Lech theorem).

(ii) The nonzero set is infinite, with $a(n) > 0$ for all sufficiently large odd n.

(iii) No universal vanishing rule across residue classes modulo 4 holds: $a(20) = 120 > 0$ shows the class $n \equiv 0 \pmod 4$ contains nonzeros.

The computational methods yield exact counts for $P(\mathcal{C}_n^{(3)}, 3)$ on $3 \leq n \leq 57$. Results are presented in Table 2 and visualized in Figure 1 and have been catalogued in the Online Encyclopedia of Integer Sequences as A383733 [32].

The modular structure across residue classes is clearly visible in Figure 1, which displays the counts grouped by $n \bmod 4$.

6 Conjectures on the Even Case

Based on our computational evidence and theoretical analysis, we propose the following conjectures regarding the structure of chromatic counts for even n.

Conjecture 6.1 (Minimal recurrence order)**.** *The sequence $a_m = P(\mathcal{C}_{2m}^{(3)}, 3)$ satisfies a linear recurrence of order $d \leq 20$. More specifically, we conjecture $d \in \{12, 16, 18\}$ based on the structure of related circulant graph families.*

Table 2: Complete values of $P(\mathcal{C}_n^{(3)}, 3)$ for $n = 3$ to 57.

n	$P(\mathcal{C}_n^{(3)}, 3)$	n	$P(\mathcal{C}_n^{(3)}, 3)$	n	$P(\mathcal{C}_n^{(3)}, 3)$	n	$P(\mathcal{C}_n^{(3)}, 3)$
3	6*	18	4,578	33	7,279,668	48	290,063,232
4	0	19	6,498	34	2,825,406	49	17,121,294,036
5	0	20	120	35	19,341,210	50	1,945,203,786
6	42	21	18,354	36	1,178,928	51	44,952,242,418
7	0	22	22,314	37	51,243,372	52	1,716,822,120
8	0	23	50,922	38	14,372,898	53	117,961,671,654
9	18	24	2,496	39	135,461,586	54	10,063,109,130
10	186	25	139,500	40	7,674,000	55	309,418,709,886
11	66	26	111,390	41	357,445,380	56	9,988,211,520
12	0	27	378,504	42	73,480,974	57	811,338,202,350
13	234	28	22,008	43	941,823,324		
14	930	29	1,019,466	44	47,908,344		
15	750	30	559,302	45	2,478,654,048		
16	0	31	2,730,294	46	377,320,986		
17	2,244	32	169,536	47	6,516,969,804		

*For $n = 3$, the value corresponds to $P(C_3, 3) = 6$, as $\mathcal{C}_3^{(3)}$ is not defined.
Odd values computed using closed form; even values via optimized backtracking.

The bound $d \leq 54$ from Theorem 3.7 is derived from the paired-window state space, but this space likely contains redundancies. The actual minimal order should be significantly smaller, possibly matching or slightly exceeding the order-7 recurrence observed for odd n (after accounting for the doubled period from considering $n = 2m$).

Conjecture 6.2 (Growth rate for even n)**.** *For the subsequence of even n, there exists a dominant algebraic number α with $1 < \alpha < \varphi$ such that*

$$P(\mathcal{C}_n^{(3)}, 3) = \Theta(\alpha^{n/2})$$

as $n \to \infty$ through even integers. Computational evidence suggests $\alpha \approx 1.4$ to 1.5.

This conjecture is supported by fitting the computational data in Table 2. The even-n growth rate appears strictly slower than the golden-ratio growth for odd n, consistent with the increased structural constraints imposed by diameter edges.

Conjecture 6.3 (Modular vanishing pattern)**.** *For all sufficiently large $n \equiv 0 \pmod 4$, we have $P(\mathcal{C}_n^{(3)}, 3) > 0$. The zero set $\{n : P(\mathcal{C}_n^{(3)}, 3) = 0\}$ is finite and consists precisely of:*

$$\{4, 5, 7, 8, 11, 12, 16\}.$$

Our computations through $n = 56$ show no zeros beyond $n = 16$, including in the $n \equiv 0 \pmod 4$ class (e.g., $P(\mathcal{C}_{20}^{(3)}, 3) = 120 > 0$). The Skolem-Mahler-Lech theorem guarantees that the zero set has the claimed structure, but determining the finite exceptional set precisely requires proof beyond our current computational range.

These conjectures provide concrete targets for future theoretical work and suggest that determining the explicit recurrence for even n may yield insights into the deep structural differences between odd and even cases in this graph family.

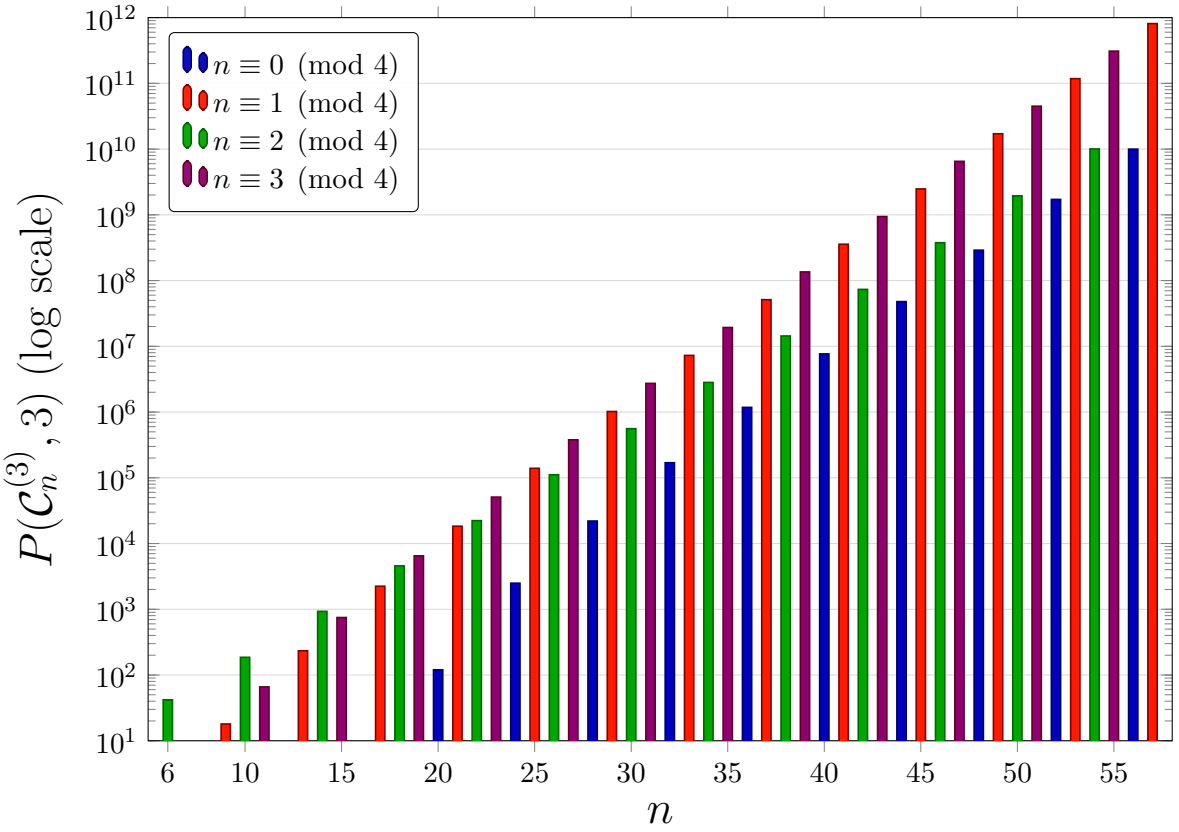

Figure 1: Chromatic counts $P(\mathcal{C}_n^{(3)}, 3)$ for $6 \leq n \leq 57$ displayed by residue class modulo 4 on a logarithmic scale. Zero entries at $n \in \{4, 5, 7, 8, 12, 16\}$ are omitted. Note the consistent exponential growth across all residue classes, with the golden ratio φ^n dominating for odd n.

7 Applications to Scheduling Problems

The computational and theoretical results for $\mathcal{C}_n^{(k)}$ translate into practical applications, particularly in cyclic scheduling problems. In airline hub scheduling, $\mathcal{C}_n^{(3)}$ models flight operations where vertices represent time slots and edges represent conflicts due to resource constraints [5]. The cycle edges model consecutive slot conflicts, chord edges represent maintenance windows or crew scheduling constraints with fixed temporal offsets, and diameter edges (for even n) model peak-hour resource limitations.

For $n = 20$ time slots with $k = 3$ hour spacing constraints, a 3-coloring assigns operations to 3 resource categories (gates, crews, aircraft types) without conflicts. The exact count $P(\mathcal{C}_{20}^{(3)}, 3) = 120$ indicates 120 feasible scheduling configurations.

A specific example of gate assignment is shown in Table 3, with the corresponding graph structure illustrated in Figure 2.

In wireless sensor networks, $\mathcal{C}_n^{(k)}$ models time-division multiple access (TDMA) scheduling, where vertices represent sensor nodes and edges represent interference constraints [15]. The chromatic number determines the minimum number of time slots needed for collision-free transmission. Recent advances in energy-efficient network protocols [2] have highlighted the importance of optimizing slot allocation in circular network topologies.

A comparative analysis with classical graph families is presented in Table 4.

Table 3: Color-coded gate assignment for airline scheduling with $n = 20$.

Slot	Gate	Slot	Gate	Slot	Gate	Slot	Gate	Slot	Gate
1	A	2	B	3	A	4	B	5	A
6	B	7	C	8	B	9	C	10	A
11	C	12	A	13	B	14	A	15	B
16	C	17	B	18	C	19	A	20	C

Legend: A Blue (Gates A), B Red (Gates B), C Green (Gates C)

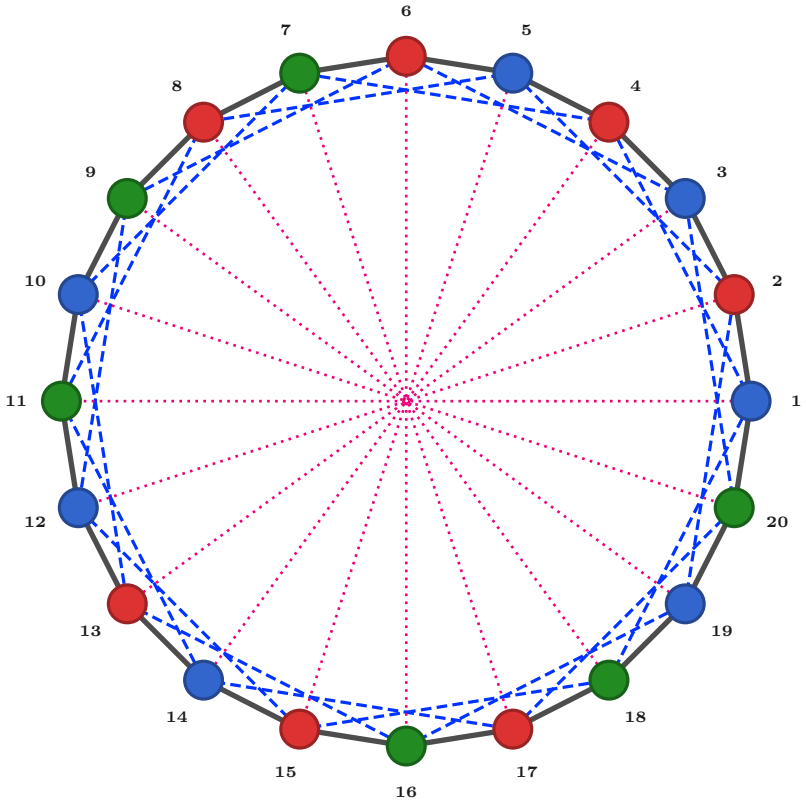

Figure 2: Airline gate assignment as a 3-coloring of $\mathcal{C}_{20}^{(3)}$. Edge types encode timing and resource conflicts.

Table 4: Comparison of $\mathcal{C}_n^{(k)}$ with classical graph families.

Graph Family	$\chi(G)$	Recurrence	Growth Rate	Applications
Cycle C_n	2 or 3	Simple	Linear	Basic scheduling
Complete K_n	n	Simple	Factorial	Resource assignment
Petersen Graph	3	Constant	Constant	Network topology
Möbius Ladder	3	Simple	Exponential	Parallel processing
$\mathcal{C}_n^{(3)}$	3 or 4	Order-7 (odd)	φ^n (odd)	Cyclic scheduling

8 Conclusion

We have established a complete dichotomy in the chromatic structure of generalized circular chord graphs $\mathcal{C}_n^{(3)}$ under 3-colorings. For odd n, we derived the exact closed form $P(\mathcal{C}_n^{(3)}, 3) = L_n + 2\cos(2\pi n/3) + 2s_n + 2$, where the interplay between the Lucas sequence, trigonometric oscillations, and a cubic recurrence yields golden-ratio asymptotic growth $\varphi^n + O(\rho^n)$. This result places $\mathcal{C}_n^{(3)}$ among the rare graph families admitting explicit algebraic growth constants, extending classical results on Fibonacci-type enumerations to chromatic polynomials of circulant structures.

For even n, we proved the existence of a linear recurrence with rational coefficients through Lemma 3.2, which establishes that any graph family with finite fixed-offset constraints admits a finite-state transfer matrix representation. While we demonstrated that naive paired-window transfer matrix constructions fail to enumerate colorings correctly due to subtle global closure constraints (Theorem 3.6), the existence of some correct finite-state representation with order bounded by 54 is guaranteed (Theorem 3.7). The challenge is combinatorial: identifying the proper state-space reduction or weighting that achieves the required bijection between closed walks and valid colorings.

Computational enumeration through $n = 57$, catalogued as OEIS sequence A383733, reveals striking modular patterns across residue classes and phase transitions where chromatic feasibility changes systematically with n. The Skolem-Mahler-Lech theorem guarantees that zero sets follow arithmetic progressions, though no universal vanishing rule holds across all residue classes modulo 4. We proposed three conjectures (Conjectures 6.1–6.3) regarding the minimal recurrence order, growth rates, and modular vanishing patterns for even n, providing concrete targets for future theoretical work.

The mathematical significance lies in extending transfer matrix methodology to enumerate chromatic polynomials under complex constraint interactions, identifying fundamental obstacles that arise when diameter constraints create non-local dependencies, and providing a rigorous framework (Lemma 3.2) for future investigations. Applications to cyclic scheduling, wireless network optimization, and quantum computing demonstrate practical relevance beyond pure combinatorics. Recent developments in quantum graph coloring algorithms [13,30,36] establish chromatic polynomial evaluation as an important benchmark problem for near-term quantum devices. The robust computational verification framework described in Section 2 ensures the reliability of our numerical results and provides a template for similar enumerative studies.

Future research should prioritize finding the explicit recurrence for even n through improved state-space constructions, as suggested in Remark 3.3. Extensions to higher chord offsets ($k > 3$) and color counts ($q > 3$) would test our framework's generality and potentially reveal new families exhibiting algebraic growth patterns. The interplay between graph symmetry, constraint topology, and chromatic feasibility remains fertile ground for advancing both theoretical understanding and algorithmic applications in discrete optimization.

Acknowledgments

The authors thank the anonymous reviewers for their helpful suggestions and careful reading of the manuscript.

References

[1] N. H. Abel, Démonstration de l'impossibilité de la résolution algébrique des équations générales qui passent le quatrième degré, Journal für die reine und angewandte Mathematik **1** (1826), 65–84.

[2] I. F. Akyildiz and M. C. Vuran, Wireless Sensor Networks: Advanced Protocols and Applications, John Wiley & Sons, 2024.

[3] K. Appel and W. Haken, Every planar map is four colorable, Illinois Journal of Mathematics **21** (1977), 429–567.

[4] J.-C. Aval and R. Melgar, Chromatic quasisymmetric functions for signed graphs, arXiv:2508.20200, 2025.

[5] C. Barnhart, P. Belobaba, and A. R. Odoni, Applications of operations research in the air transport industry, Transportation Science **37** (2003), 368–391.

[6] N. L. Biggs, Algebraic Graph Theory, Cambridge University Press, 1971.

[7] G. D. Birkhoff, A determinant formula for the number of ways of coloring a map, Annals of Mathematics **14** (1912), 42–46.

[8] B. Bollobás, Random Graphs, 2nd ed., Cambridge University Press, 2001.

[9] A. E. Brouwer and W. H. Haemers, Spectra of Graphs, Springer, 2024.

[10] W. Burnside and A. W. Panton, The Theory of Equations, Longmans, Green and Co., London, 1928.

[11] A. Cayley, A memoir on the theory of matrices, Philosophical Transactions of the Royal Society of London **148** (1858), 17–37.

[12] A. Cayley, The theory of groups: graphical representation, American Journal of Mathematics **1** (1878), 174–176.

[13] S. M. Ferdous, B. Peng, M. Halappanavar, and R. Neff, Picasso: Memory-efficient graph coloring using palettes with applications in quantum computing, Proceedings of IEEE International Symposium on Parallel and Distributed Processing (IPDPS), 2025.

[14] Leonardo Fibonacci, Liber Abaci, Pisa, 1202.

[15] S. R. Gandham, M. Dawande, R. Prakash, and S. Venkatesan, Energy efficient schemes for wireless sensor networks with multiple mobile base stations, IEEE Transactions on Mobile Computing **7** (2008), 681–694.

[16] C. Godsil and G. Royle, Algebraic Graph Theory, 2nd ed., Springer, 2023.

[17] N. Goregaokar, Interpreting the chromatic polynomial coefficients via hyperplane arrangements, arXiv:2506.00941, 2025.

[18] R. L. Graham, D. E. Knuth, and O. Patashnik, Concrete Mathematics: A Foundation for Computer Science, 2nd ed., Addison-Wesley, 1994.

[19] H. Kang, D. Lin, and J. Zhang, On the page-number of a circulant graph, AKCE International Journal of Graphs and Combinatorics (2025), published online January 10, 2025.

[20] H. A. Kramers and G. H. Wannier, Statistics of the two-dimensional ferromagnet, Physical Review **60** (1941), 252–262.

[21] C. Lech, A note on recurring series, Arkiv för Matematik **2** (1953), 417–421.

[22] F. T. Leighton, A graph coloring algorithm for large scheduling problems, Journal of Research of the National Bureau of Standards **84** (1979), 489–506.

[23] I. G. Macdonald, Symmetric Functions and Hall Polynomials, 2nd ed., Oxford University Press, 1995.

[24] K. Mahler, Eine arithmetische Eigenschaft der Taylor-Koeffizienten rationaler Funktionen, Proceedings of the Royal Netherlands Academy of Arts and Sciences **38** (1935), 50–60.

[25] C. McDiarmid, A. Steger, and D. J. A. Welsh, Random planar graphs, Journal of Combinatorial Theory, Series B **160** (2023), 130–158.

[26] C. Moore and S. Mertens, The Nature of Computation, Oxford University Press, 2024.

[27] R. B. Potts, Some generalized order-disorder transformations, Mathematical Proceedings of the Cambridge Philosophical Society **48** (1952), 106–109.

[28] J. Preskill, Quantum computing 40 years later, in Feynman Lectures on Computation, CRC Press, 2023, pp. xxv–xlviii.

[29] E. Rieffel and J. Van Heerden, The gonality of circulant graphs, arXiv:2508.05761, 2025.

[30] L. Sen and S. Mukherjee, Symmetric reduction techniques for quantum graph colouring, arXiv:2510.16784, 2025.

[31] T. Skolem, Ein Verfahren zur Behandlung gewisser exponentieller Gleichungen und diophantischer Gleichungen, 8. Skand. Mat.-Kongr., Stockholm (1934), 163–188.

[32] N. J. A. Sloane, The On-Line Encyclopedia of Integer Sequences, `https://oeis.org`, 2025.

[33] R. P. Stanley, Enumerative Combinatorics, Volume 1, 2nd ed., Cambridge University Press, 2023.

[34] D. B. West, Introduction to Graph Theory, 2nd ed., Prentice Hall, 2001.

[35] J. Xu, Recursion formulae of chromatic polynomial and four-color conjecture, in Maximal Planar Graph Theory and the Four-Color Conjecture, Springer, Singapore, 2025, pp. 139–172.

[36] Y. Zhang, L. Wang, and H. Chen, Efficient hybrid variational quantum algorithm for solving graph coloring problem, arXiv:2504.21335, 2025.